pH-Based Regulation of Hydrogel Mechanical Properties Through Mussel-Inspired Chemistry and Processing

*Devin G. Barrett, Dominic E. Fullenkamp, Lihong He, Niels Holten-Andersen, Ka Yee C. Lee, and Phillip B. Messersmith**

The mechanical holdfast of the mussel, the byssus, is processed at acidic pH yet functions at alkaline pH. Byssi are enriched in Fe^{3+} and catechol-containing proteins, species with chemical interactions that vary widely over the pH range of byssal processing. Currently, the link between pH, Fe^{3+}-catechol reactions, and mechanical function is poorly understood. Herein, it is described how pH influences the mechanical performance of materials formed by reacting synthetic catechol polymers with Fe^{3+}. Processing Fe^{3+}-catechol polymer materials through a mussel-mimetic acidic-to-alkaline pH change leads to mechanically tough materials based on a covalent network fortified by sacrificial Fe^{3+}-catechol coordination bonds. These findings offer the first direct evidence of Fe^{3+}-induced covalent cross-linking of catechol polymers, reveal additional insight into the pH dependence and mechanical role of Fe^{3+}-catechol interactions in mussel byssi, and illustrate the wide range of physical properties accessible in synthetic materials through mimicry of mussel-protein chemistry and processing.

1. Introduction

Load-bearing biological materials serve as valuable models for designing synthetic materials with extraordinary mechanical properties.[1–3] This process often begins with observations of interesting physical properties of tissues followed by identification of essential elements or building blocks. However, biologically inspired design is most enabling when there exists an understanding of the basic chemical and physical principles underlying the structure-function relationships, including tissue-processing/fabrication strategies in biological systems.[4–6] Spider dragline silk and mussel byssi are two examples of fibrous biological tissues with overtly mechanical functions that have attracted great interest among researchers due to their exceptional material properties and vast potential for applications.[7,8] In the case of spider silk, the protein building blocks were described many years before key features of silk-fiber spinning were known.[9–11] One recently uncovered feature of silk-fiber processing is the apparent acidification of the duct lumen during spinning,[12] which is believed to play a role in protein condensation, assembly, and fiber formation from soluble precursors.[13,14]

pH regulation is also employed by marine organisms during secretion of attachment structures.[15] The mussel byssus is a proteinaceous and acellular holdfast composed of a collection of byssal threads tethering the organism to a surface. Many mussel species inhabit turbulent intertidal zones by relying on byssal threads that are strong, resilient, and designed to resist damage and detachment.[16–21] The byssus is molded from liquid protein precursors whose pH during early secretion is initially acidic (pH ≈ 5.8);[22] after formation of the byssus and exposure to sea water, the adhesive structure equilibrates to marine pH (≈8.5). While the byssus is primarily composed of organic macromolecules, it has been shown to be enriched in inorganic elements such as Fe^{3+},[23] and its remarkable mechanical properties have been hypothesized to originate from both inorganic (metal coordination) and organic (covalent) bonds.[19–21,24] For example, the ability of the byssus to 'self-heal' after suffering apparently non-recoverable mechanical deformation[19] is thought to be related to coordination bonds formed between metals and byssal proteins.[20,21,24] Although there is a growing effort to develop

Dr. D. G. Barrett
Biomedical Engineering Department
Chemistry of Life Processes Institute
Institute for Bionanotechnology in Medicine
Northwestern University
Evanston, IL 60208, USA
Dr. D. E. Fullenkamp, Dr. L. He
Biomedical Engineering Department
Chemistry of Life Processes Institute
Northwestern University, Evanston, IL 60208, USA
Dr. N. Holten-Andersen, Prof. K. Y. C. Lee
Chemistry Department
Institute for Biophysical Dynamics
James Franck Institute, University of Chicago
Chicago, IL 60637, USA
Prof. P. B. Messersmith
Biomedical Engineering Department
Materials Science and Engineering Department
Chemical and Biological Engineering Department
Chemistry of Life Processes Institute
Institute for Bionanotechnology in Medicine
Robert H. Lurie Comprehensive Cancer Center
Northwestern University, Evanston, IL 60208, USA
E-mail: philm@northwestern.edu

DOI: 10.1002/adfm.201201922

synthetic materials inspired by mussel byssal proteins and threads,[8,25–28] mimicry of mussel byssal processing is still in the early stages.[29–31]

The complex mechanochemical interactions between Fe^{3+} and catechols during and after byssal formation are the particular focus of this work. The catechol-containing residue 3,4-dihydroxy-L-phenylalanine (DOPA) is found in most byssal proteins, and previous studies have shown that Fe^{3+}-catechol coordination interactions are mechanically active.[24,30,32–34] While multiple reports have recently compared gels cross-linked by oxidative covalent coupling and catechol coordination of Fe^{3+}, the interplay between these curing mechanisms is poorly understood.[30,34] This topic should be further investigated due to the complex interactions between Fe^{3+} and catechols; spectroscopic evidence has linked the presence of Fe^{3+} to catechol oxidation,[35,36] and speculation exists about the possible involvement of Fe^{3+} in formation of covalent DOPA-DOPA linkages.[37]

In this report, we show that reactions between Fe^{3+} and catechol polymers are strongly dependent upon pH, with covalent catechol-catechol linkages and Fe^{3+}-catechol coordination dominating at acidic and basic conditions, respectively. The mechanical effects of such diverse reaction products were studied in model polymer hydrogels by using pH to regulate the balance of covalent and coordination bonds in, and therefore the viscoelastic character of, the gel network. Finally, mimicking the acidic-to-basic pH switch that occurs during byssus formation in our synthetic system led to covalent gel networks that were mechanically augmented by Fe^{3+}-catechol coordination bonds. In these networks, Fe^{3+}-catechol coordination bonds dissipate energy through rupture but rapidly re-form to regenerate the original mechanical properties during subsequent loading cycles, functioning as sacrificial bonds in analogy to those that are such prominent features of structural biological tissues.[38,39]

2. Cross-Linking of Monofunctional Catechol Polymers: Influence of [Fe^{3+}] and pH

We first investigated the interactions between Fe^{3+} and a monofunctional catechol-containing poly(ethylene glycol) (PEG) polymer (mPEG-cat; ≈5 kDa; **Figure 1**) in order to understand the impact of pH and Fe^{3+}:catechol stoichiometry on the formation of the covalent polymerization products. The use of mPEG-cat allowed gel-permeation chromatography (GPC)

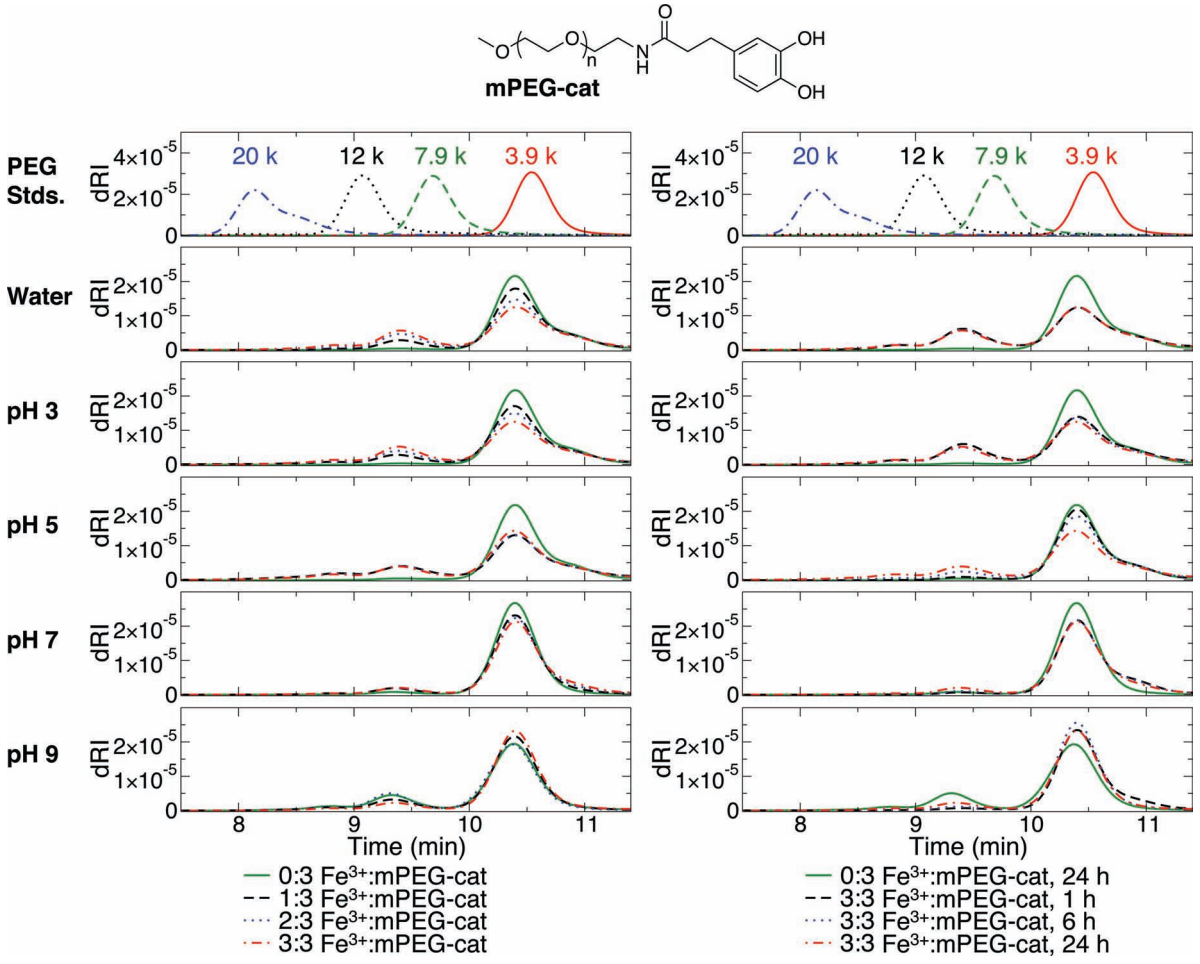

Figure 1. GPC data of mPEG-cat (top) after 24 h incubation with Fe^{3+} (left) and time dependence of the reaction with Fe^{3+} (right). The monomers and multimers elute at ≈10–11 min and ≈8.5–10 min, respectively.

experiments to be performed with similar end-group concentrations and buffer conditions used for gel studies (described below), but without the complications associated with network formation. As shown in Figure 1, at pH ≤ 3, GPC traces reveal increased multimer formation, with a linear dependence on the Fe^{3+}:catechol ratio (Supporting Information, Figure S1a). At pH ≤ 3 and an Fe^{3+}:catechol ratio of 3:3, the reaction is complete after 1 h, and reaction mixtures contained ≈30% multimers, with the dominant species being the mPEG-cat dimer (Figure 1 and Supporting Information, Figure S1b).

The GPC studies of mPEG-cat with Fe^{3+} at pH 5 revealed a surprisingly high degree of mPEG-cat polymerization after 24 h (Figure 1; Supporting Information, Figure S1). This result was unexpected, as visual inspection of a mixture of the polyfunctional, catechol-containing 8cPEGa (8-arm, catechol-modified PEG with amide linkages) (**Figure 2**) with Fe^{3+} under similar

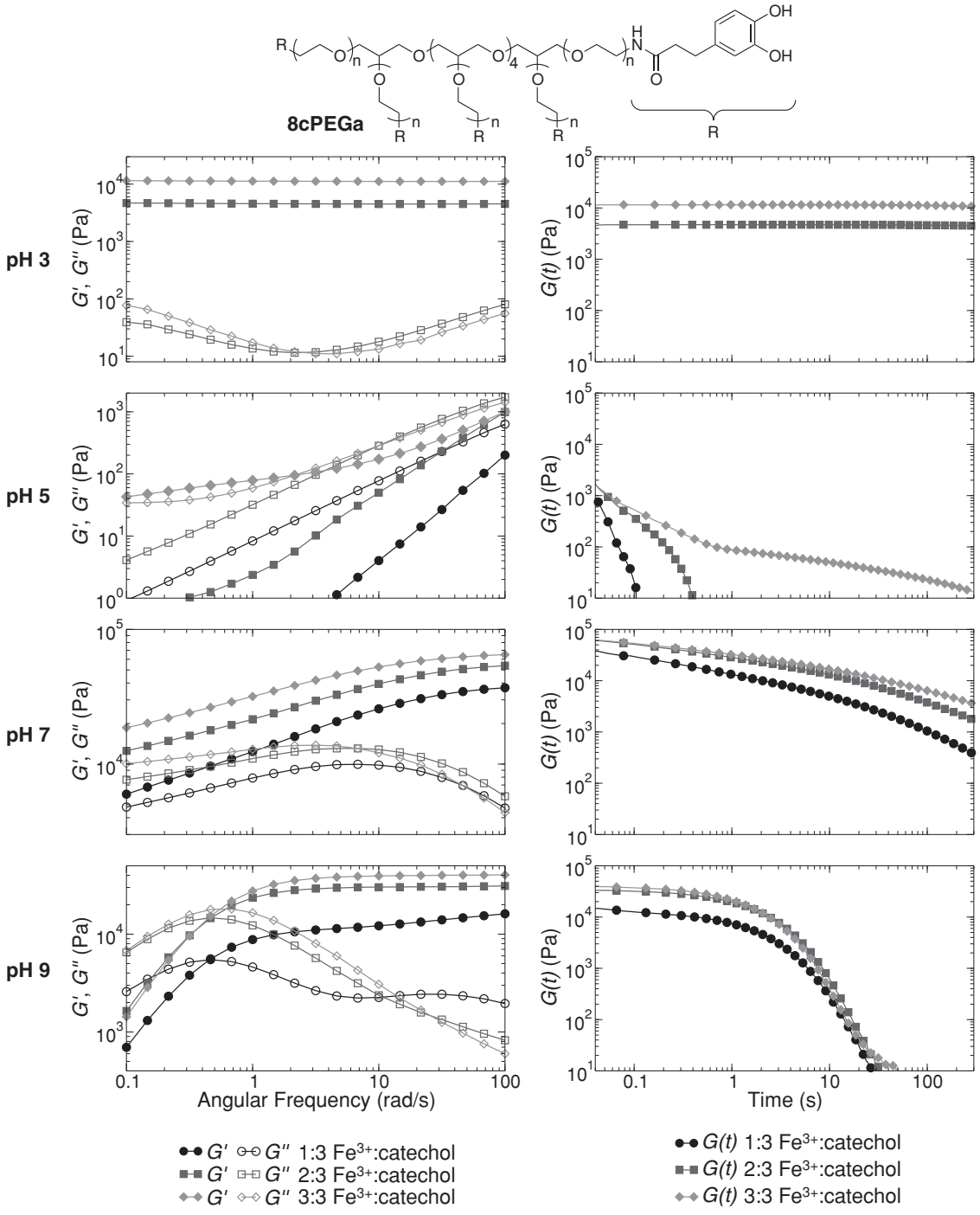

Figure 2. Frequency sweep (left) and step-strain (right) characterizations of hydrogels composed of 8cPEGa (top) and Fe^{3+} at pH 3, 5, 7, and 9.

conditions revealed no gel formation, as determined by vial inversion. We also found that the reaction at pH 5 was not significantly dependent on the Fe^{3+}:catechol ratio, as the sample with a ratio of 1:3 produced an essentially equivalent amount of multimers as the sample with a ratio of 3:3. Interestingly, the time-dependence of the reaction at pH 5 (Supporting Information, Figure S1b) showed that polymerization occurred slowly and only resulted in significant multimer formation after several hours. The GPC results for the reactions at pH 7 were qualitatively similar to those at pH 5, although the cross-linking reaction appeared to be slower. After 24 h of reaction at pH 7, all of the mPEG-cat solutions with Fe^{3+} contained ≈10% multimer, compared with ≈25–30% for the reactions at pH 5. From these data, we can say that the extent and rate of covalent polymerization of catechols by Fe^{3+} are highest at low pH and decrease as neutral pH is approached.

The GPC results at pH 9 were unique because of the significant presence of multimers after 24 h in the absence of Fe^{3+}, a result we attribute to the auto-oxidation of catechols in the basic conditions. Multimer formation at pH 9 proceeded slowly and decreased as the Fe^{3+}:catechol ratio increased (Figure 1 and Supporting Information, Figure S1). The inverse relationship between the multimer formation and the Fe^{3+}:catechol ratio suggests that Fe^{3+} serves a protective role against the auto-oxidation of catechols at basic pH,[40] although we cannot exclude a minor suppression of auto-oxidation as a result of the slight acidification associated with the added Fe^{3+} (the strong acidity of $FeCl_3$ slightly depressed the pH of the buffered reaction solutions; see Supporting Information, Table S1).

mPEG-cat was also used to study the presence of coordination bonds by UV–vis spectroscopy, the standard method of characterizing these linkages. The interactions between catechols and Fe^{3+} are known to produce signature colors as a function of pH.[30] When Fe^{3+} and mPEG-cat (molar ratio of 2:3) were combined at pH 3, 5, 7, and 9, the solutions became green, blue, purple, and red (Supporting Information, Figure S2). These results correspond well with the coordination-based hydrogels described by Holten-Andersen and colleagues.[30] Further, in anticipation of novel hydrogels to be designed later, we incubated Fe^{3+} and mPEG-cat (molar ratio of 2:3) at pH 3 for 2 h; during this time, the samples turned green, as expected. These solutions were then subjected to an increase in alkalinity to pH 7 or 9; again, the samples changed color, to purple or red, respectively. An adjustment to pH 5 was not possible due to the inability to overwhelm the pH 3 buffer without overly diluting the coordinating species. Taken together, these results suggest that catechol systems are able to coordinate Fe^{3+} at elevated pH, including after a period of covalent oligomerization in acidic conditions.

3. Properties of Catechol-Polymer Gels: Influence of [Fe^{3+}] and pH

The Fe^{3+}-induced gel formation of a polyfunctional, catechol-terminated PEG (8cPEGa) was characterized both as a function of pH and Fe^{3+}:catechol ratio. The covalent gels rapidly formed (<1 min) in unbuffered water (pH ≈ 2) at an Fe^{3+}:catechol ratio of 2:3 (Supporting Information, Figure S3). These hydrogels appeared to be elastic solids, with G' and G'' displaying essentially frequency-independent behavior and $G' >> G''$. The mechanical properties are similar in modulus and yield strain to other catechol-modified PEG hydrogels formed by covalent cross-linking with $NaIO_4$.[27,41] The ability of Fe^{3+} to oxidize these polymers rapidly and cross-link them covalently at low pH is consistent with our GPC studies (Figure 1). Hydrogels also formed at an Fe^{3+}:catechol ratio of 3:3, though these gels formed too rapidly to be inserted into our rheometer prior to gelation. Solutions with an Fe^{3+}:catechol ratio of 1:3 in unbuffered water did not form gels (Supporting Information, Figure S3), likely due to insufficient cross-linking for network percolation.

Next, we studied gel formation in buffered systems in order to probe the hydrogel mechanical properties as a function of pH and Fe^{3+}:catechol ratio. The gelation times at various cross-linking conditions are documented in the Table S2 in the Supporting Information. As judged by vial inversion, gels formed more slowly at acidic pH compared to those cross-linked at alkaline pH. While gels did not form within 60 min at pH 5, these solutions immediately became more viscous upon mixing 8cPEGa and Fe^{3+}.

To differentiate between covalent- and coordination-based cross-linking, gels were further studied by rheology. Gels did not form at pH 3 for an Fe^{3+}:catechol ratio of 1:3. For larger Fe^{3+}:catechol ratios, we saw mechanical properties that are typical of elastic solids and similar to that of gels formed in unbuffered water (Figure 2 and Supporting Information, Figure S4). Step-strain measurements show the relaxation time to be essentially infinite, consistent with a covalently gelled network. Additionally, the modulus of gels formed at pH 3 increased at higher Fe^{3+}:catechol ratios, which is consistent with a higher cross-linking density.

At pH 9, materials displaying Maxwell like relaxation behavior were formed in the presence of Fe^{3+}. This behavior reflects the coordination cross-linking, likely in a bis- or tris-catecholate configuration, and is consistent with the previous report of Holten-Andersen et al.[30] Interestingly, gels formed with an Fe^{3+}:catechol ratio of 3:3 were stiffer at high frequency than those formed with a ratio of 1:3 or 2:3. This result is not intuitive, as one would expect equimolar amounts of Fe^{3+} and catechol end-groups to soften the gel by forming monocatecholate species, thus preventing coordination-based cross-linking that must proceed through bis- and tris-catecholate motifs.

Hydrogels formed at pH values between 5 and 7 displayed very different material properties. As shown in Figure 2, gels formed at pH 5 are simply viscous liquids with relatively short relaxation times; this observation is in stark contrast to both the essentially infinite relaxation times of covalent gels formed at pH 3 and the Maxwell like behavior of coordination-dominated gels formed at pH 9. At pH 7, unexpected material properties were observed. As demonstrated by past equilibrium titration studies of Fe^{3+}-catechol solutions[40] and our own GPC studies, neither covalent nor coordination cross-linking is expected to be especially dominant at pH 7. Fe^{3+}-mediated oxidative oligomerization is not very efficient at pH 7, and a significant fraction of terminal catechols are not expected to participate in network formation through coordination of Fe^{3+}. However, surprisingly rigid materials resulted when gels were formed at pH 7. Not only were the moduli of the gels formed at pH 7 greater than those of materials formed at pH 9, but also the gel relaxation times under

these conditions were clearly longer than those formed at pH 9, as no crossover is seen in the frequency sweep at pH 7 (Figure 2). We are currently investigating why pH 7 gels have significantly longer relaxation times than pH 9 gels. We hypothesize that the higher hydroxide concentration at pH 9 may increase the bond-relaxation rate, though a role for the buffer or the amount of covalent cross-linking cannot be ruled out at this time. In order to further investigate the balance of covalent and coordination bonds in these materials, their stabilities in solutions of ethylenediaminetetra-acetic acid (EDTA) was monitored (Supporting Information, Figure S5, Supporting Information, Table S3). The samples designed at pH 3 were stable in EDTA, while hydrogels fabricated at pH 5, 7, and 9 almost entirely dissolved when they were exposed to EDTA. These data qualitatively support our interpretation of the rheological data.

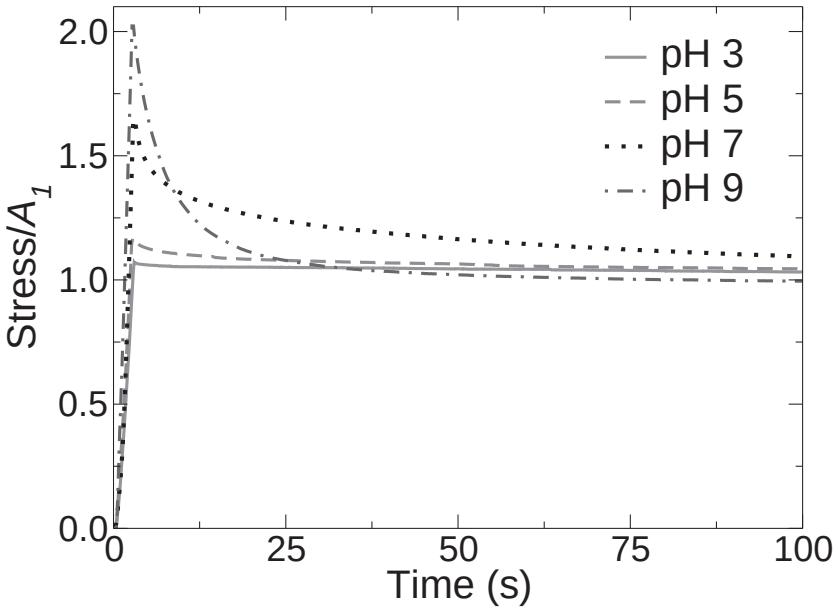

Figure 3. pH-dependent relaxation of mussel-inspired hydrogels containing covalent and coordination bonds. Samples were formed at pH = 3 and then equilibrated to the pH values indicated before testing in compression. The samples were strained to 20%, and the stress was monitored for 100 s. A_1 represents the steady-state stress.

Taken together, these results suggest that covalent cross-linking plays a very significant role at pH 3 and a lesser role at pH 5, 7, and 9. To the best of our knowledge, our GPC results showing mPEG-cat multimers are the first direct evidence of oxidative catechol oligomerization by Fe^{3+}. Though no direct evidence of this reaction has been previously described, spectroscopic results have shown that catechols can be oxidized to the *o*-quinone form by Fe^{3+}.[35,36] Additionally, a hypothesis that Fe^{3+} serves as an inorganic oxidant leading to byssal protein cross-linking has been proposed.[37] Our GPC experiments, albeit using a fully synthetic model polymer, support this hypothesis and provide the first direct evidence of covalent reaction products. These findings warrant further studies as to whether or not Fe^{3+}, which is enriched in mussel adhesives relative to seawater,[42] acts as an inorganic oxidant for formation of byssal threads.

4. Mimicking the pH Increase of Byssal Processing

As previously stated, during byssal processing, liquid protein precursors are secreted at acidic pH[22] and rapidly equilibrate to alkaline marine pH (≈8.5) when exposed to seawater. Motivated in part by the use of pH regulation by the mussel and that our findings show pH-dependent Fe^{3+}-catechol interactions, we sought to create functional materials that exhibit exceptional mechanical properties through mussel-inspired pH processing. Thus, Fe^{3+}-catechol polymer hydrogels were formed for 24 h at pH 3 with an Fe^{3+}:catechol ratio of 2:3, and were then immersed for 24 h in a buffer at pH 3, 5, 7, or 9. The first step of this approach imparted an initial and equivalent covalent network in all of the samples, allowing us to then probe the mechanical contribution of the Fe^{3+}-catechol coordination bonds that are expected to occur upon equilibration at a higher pH.

In the first experiment, the hydrogels were strained in compression by 5, 10, or 20% and the evolution of the stress was monitored for 100 s (**Figure 3**, Supporting Information, Figure S6). The discussion here will focus on samples strained at 20%, however the trends mirror those observed at 5% and 10% strain (Supporting Information, Table S4). The modulus, amount of relaxation, and relaxation rate were strongly dependent on the equilibration pH. Extraction of the initial and steady-state moduli from the relaxation curves revealed an increase in modulus with increasing pH (**Figure 4**). The hydrogels equilibrated at pH 3, 5, 7, and 9 dissipated 3.3%, 9.7%, 32.3%, and 51.2% of the maximum stress, respectively. The relaxation times were calculated to be approximately 25 s for pH 5, 18 s for pH 7, and 5 s for pH 9 (Figure 4); no relaxation times were determined for materials equilibrated at pH 3 due to the presence of a primarily covalent gel network.

In the second experiment, samples were cycled through compression loops with increasing strain (10%, 20%, 40%, 60%, 70%, 80%), allowing us to monitor the effect of the equilibration pH on mechanical recovery (**Figure 5**). A qualitative trend observed in these data is the increase in compression modulus with increasing equilibration pH, which is consistent with the results of stress-relaxation experiments (Figure 4) and can be attributed to augmentation of the covalent network by Fe^{3+}-catechol coordination bonds, which are much more prevalent at high pH. Notably, gels equilibrated at pH 9 sustained the largest stress (≈260 kPa) and strain values (80%) without suffering permanent damage. A prominent feature in the compression loops was the presence of hysteresis between the loading and unloading curves. Minimal hysteresis was observed for the gels equilibrated at pH 3 and 5. However, substantial hysteresis was observed in the samples equilibrated at pH 7 and 9, reflecting energy dissipation by the rupture of the Fe^{3+}-catechol coordination bonds. Presumably, the ruptured coordination bonds rapidly re-form, as the loading curves from successive

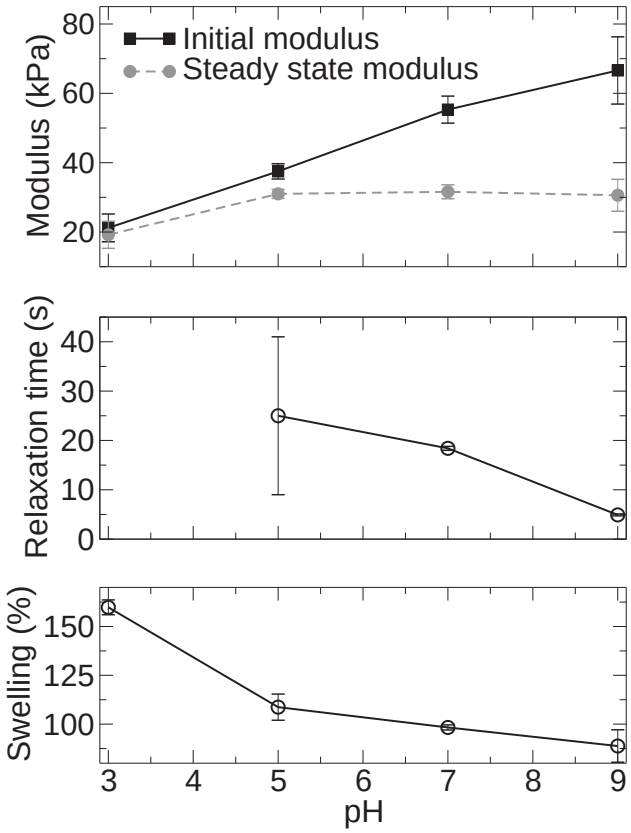

Figure 4. Physical characterization of mussel-inspired gels formed at pH = 3 and then equilibrated at pH = 3–9. The initial and steady-state moduli demonstrate pH-dependent differences due to the presence of coordination bonds and their ability to dissipate energy (top panel). The relaxation times (center panel) and swelling (bottom panel) decrease with increasing pH. The relaxation times for the gels both as-formed and equilibrated at pH = 3 are not shown, as it was essentially infinite.

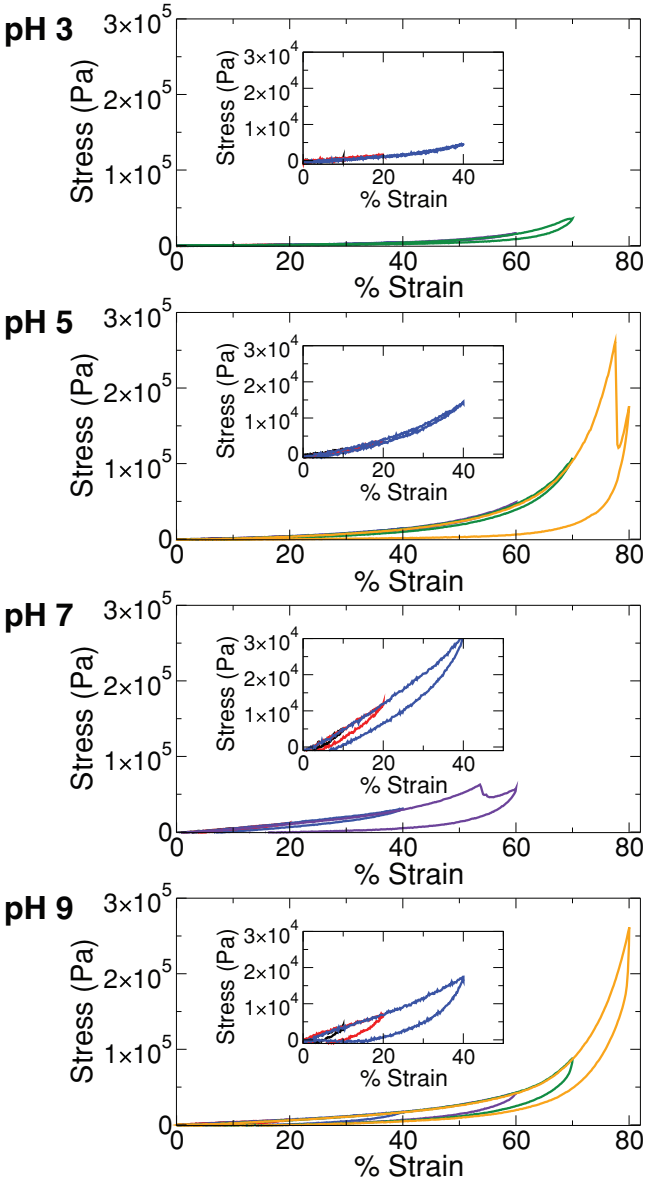

Figure 5. Representative stress–strain curves of gels formed by mussel-mimetic processing involving initial cross-linking at pH = 3 and then equilibration to the pH values indicated. The samples were deformed in multiple compression cycles, where the strain was successively increased to 10% (black), 20% (red), 40% (blue), 60% (purple), 70% (green), and 80% (yellow). In the case of the materials equilibrated at pH = 7, the final two loops were unnecessary due to failure at ≈55% strain. The insets show the detail in the low-strain regime (0–50%).

compression loops with increasing strain were nearly perfectly overlapping (Figure 5).

Covalently cross-linked hydrogels are essentially Hookean elastic materials at low strains, acting like springs that store energy without dissipation. Fe^{3+}-catechol gels equilibrated at pH 3 fit this description due to their purely covalent nature (no Fe^{3+}-catechol coordination bonds should form at such acidic pH). In contrast, the relaxation and hysteresis observed in gels equilibrated at pH 7 and 9 are attributed to the presence of mechanically functional Fe^{3+}-catechol coordination bonds (Figure 5, **Scheme 1**). Even at low strain, these gels displayed mechanical hysteresis between loading and unloading curves. Such a viscoelastic behavior is reminiscent of the relaxation and hysteresis observed in recently reported synthetic muscle-mimetic biomaterials, which were designed to exhibit high toughness and resilience reminiscent of native tissues by incorporating secondary and tertiary structures that dissipate energy under applied force.[43] This viscoelasticity is also a characteristic feature of biological materials like tendons and cartilage,[38,39] where it plays an important role in transferring and mitigating loads between soft and hard tissues.

Non-covalent interactions within and between the macromolecular constituents often play key roles in defining the mechanical properties of biological tissues.[19–21,24,44–47] For example, non-covalent interactions act in a sacrificial manner under applied loads by temporarily dissociating to dissipate energy and reveal hidden length, thereby enhancing toughness and preventing catastrophic material failure caused by the rupture of covalent bonds.[48] Because of their dynamic nature, such

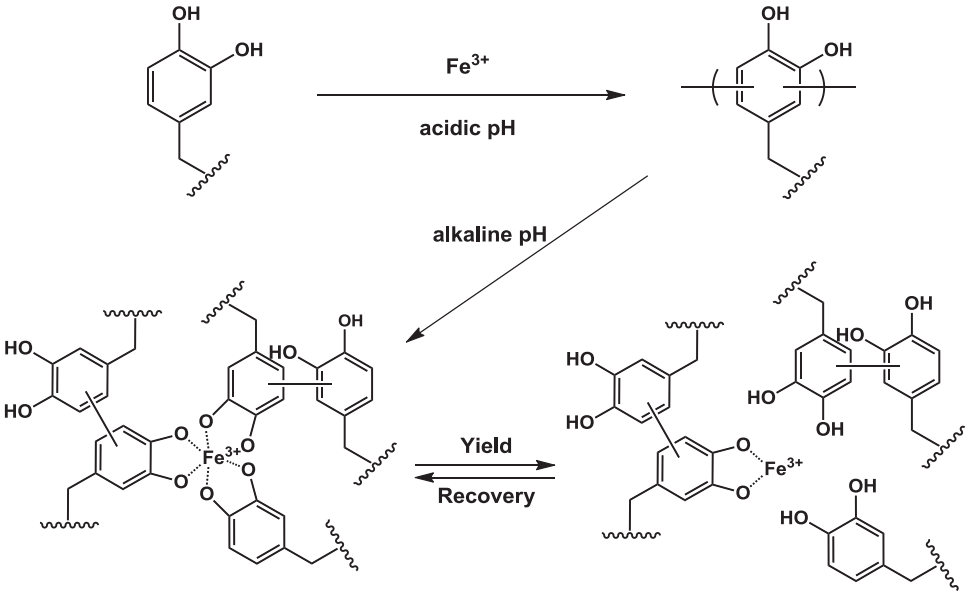

Scheme 1. Proposed pH dependence of covalent- and coordination-bond formation in catechol-polymer hydrogels containing Fe^{3+}. The reaction of the catechol-terminated branched PEG with Fe^{3+} at acidic pH results in covalently cross-linked hydrogels. Subsequent equilibration of these gels at pH = 5, 7, or 9 introduces varying amounts of Fe^{3+}-catechol coordination bonds that mechanically enhance the covalent network. Under the influence of a mechanical force, these coordination bonds reversibly rupture and re-form, acting as a mechanism for energy dissipation. Both oligomeric and monomeric (unreacted) catechols are believed to participate in the coordination network.

bonds can re-form to recover all or part of the original mechanical properties when the external load is removed.[19–21,44–46] Purely synthetic materials have been designed with covalent networks strengthened by non-covalent interactions, such as hydrophobic bonds[49,50] and hydrogen bonding,[51–53] in an analogous way to achieve unique physical properties. Metal coordination interactions appear to have this function also, as illustrated here and by others.[30,54]

Finally, these experiments have revealed new details of Fe^{3+}-catechol mechanochemistry, including a direct demonstration of Fe^{3+}-based oxidative oligomerization of catechols, the pH dependence of this reaction, and the mechanical consequences of covalent and coordination cross-links arising in Fe^{3+}-containing catechol polymer systems. Our findings have important implications for understanding the processing and properties of the mussel byssus, with the conceptual scheme shown in Scheme 1 serving as a template for a more-complete hypothesis on the mechanical function of Fe^{3+} in the mussel byssus. We postulate that co-secretion of Fe^{3+} with DOPA-containing proteins, which occurs at acidic pH, gives rise to limited formation of a covalent network during byssus molding. Subsequent exposure to alkaline seawater increases the pH into the range where Fe^{3+}-catechol coordination bonds are favored, and these bonds confer unique mechanical properties associated with their dynamic ability to rupture and re-form. Although the findings for the model polymer system reported herein support this dual role for Fe^{3+}, further studies will be needed to examine if the mussel employs this mechanism for optimal mechanical performance of byssal threads.

5. Conclusions

This work demonstrates a new bioinspired strategy for designing remarkably tough hydrogels. By regulating the pH of the reaction between catechol-terminated branched PEG and Fe^{3+}, a covalently cross-linked network was fortified with a series of coordination bonds, which act as sacrificial and reversible interactions to dissipate energy during deformation. With respect to opportunities related to the design of novel biologically inspired materials, our findings illustrate the richness of the cross-linking chemistries and physical properties accessible in synthetic mussel-inspired materials, achieved through facile manipulation of pH, composition, and processing. Careful management of these variables affords access to a broad spectrum of physical properties reflecting the balance of covalent and coordination cross-linking in the gel network. These hydrogels, with a viscoelastic response and a water content reminiscent of hydrated biological soft tissues, represent a novel class of mussel-mimetic biomaterials inspired in both content and processing.

6. Experimental Section

Materials: Acetic acid, bicine, bis-Tris, bis-Tris hydrochloride, 3-(3,4-dihydroxyphenyl)propionic acid (DHPA), dichloromethane (DCM), dimethylformamide (DMF), EDTA disodium salt dihydrate, ferric chloride hexahydrate, formic acid, sodium acetate trihydrate, sodium formate, and triethyleamine (TEA) were purchased from Sigma Aldrich (Milwaukee, WI). The PEG products – linear, monofunctional, amine-terminated PEG (mPEG-NH_3Cl; MW 5000 g mol^{-1}) and 8-arm amine-terminated PEG (8PEG-NH_3Cl; hexaglycerin core; MW 20 000 g mol^{-1}) – were purchased from JenKem Technology USA Inc. (Allen, TX). *N*-hydroxybenzotriazole (HOBt) was purchased from Advanced ChemTech (Louisville, KY). 2-(1H-benzotriazole-1-yl)-1,1,3,3-tetramethyluronium hexafluorophosphate (HBTU) was purchased from EMD Chemicals (Gibbstown, NJ). All of the chemicals were used without further purification.

Synthesis of mPEG-cat: Monofunctional, amine-terminated PEG (0.6 mmol, MW 5000 g mol^{-1}) was dissolved in DCM (10 mL). DHPA (1.2 mmol), HOBt (1.98 mmol), HBTU (1.2 mmol), and TEA (1.98 mmol) were sequentially added to this solution. Afterwards, DMF (5.0 mL) was added to help dissolve all of the reagents, and this coupling reaction was carried out at 20 °C under N_2 with continuous stirring for 2.0 h. The crude product was purified by precipitation in 300 mL of diethyl ether (1×) and in 300 mL of acidified methanol (3×) at –20 °C. After one additional precipitation in diethyl ether, the mPEG-cat was dried under vacuum (≈90% conversion).

Fe^{3+}-Based Oligomerization of mPEG-cat as Studied by GPC: The reaction between mPEG-cat ($M_n \approx 5600$ Da by MALDI-TOF-MS) and Fe^{3+} was performed in buffered and unbuffered water. When the reaction was performed in unbuffered water, the pH was 2–3 due to the acidity of the $FeCl_3$. Buffers (500 mM) of formate, acetate, bis-tris, and bicine were used to control the pH of the solutions at pH 3, 5, 7, and 9, respectively. Aliquots of 3.0 mg of mPEG-cat were dissolved into 7.14 µL of water or buffer. Freshly prepared 100 mM, 200 mM, or 300 mM $FeCl_3$ solutions (1.79 µL) were added to each solution of mPEG-cat to produce Fe^{3+}:catechol ratios of 1:3, 2:3, or 3:3, respectively. For the 0× Fe^{3+} samples, 8.93 µL of water or buffer were added to dissolve the polymer. The final reaction concentration of mPEG-cat was 60 mM (replicating the catechol concentration in the gel studies). After 24 h, 6 h, or 1 h, 100 mM EDTA (10× EDTA relative to Fe^{3+}) was added to the samples to sequester the Fe^{3+}. The samples were further diluted to 10 mg mL^{-1} with the GPC buffer (50 mM citrate, 100 mM $NaSO_4$, pH 3.5). Each sample (10 µL) was injected into an Agilent 1100 Series high-performance liquid chromatography (HPLC) unit (flow rate 1.0 mL min^{-1}) equipped with a Shodex KW-803 GPC column (heated to 40 °C) and inline with Wyatt Dawn Heleos II and Optilab T-rEx dRI detectors. PEG standards (Varian) of 3930, 7920, 12 140, and 21 030 Da were prepared in GPC buffer at 10 mg mL^{-1}. Wyatt Astra software was used to calculate M_n, M_w, and the relative percentages of monomer vs. multimers of mPEG-cat. The PEG dn/dc was taken to be 0.136 mL g^{-1}.

UV–vis Spectroscopy with mPEG-cat and Fe^{3+}: UV–vis data were recorded on a Shimadzu BioSpec-nano spectrophotometer. mPEG-cat was dissolved in buffer (pH 3, 5, 7, or 9), and Fe^{3+} was added such that the final polymer concentration was 30% and the Fe^{3+}:catechol ratio was 2:3. Solutions were diluted with buffer until the absorbance was less than 1. Alternatively, samples were prepared by combining mPEG-cat at pH 3 for 2 h and then diluting the solutions with buffer of elevated pH.

Synthesis of 8cPEGa: Each of the following components was completely dissolved in 75 mL of 1:2 DCM:DMF in succession before additional reagents were added: 8PEG-NH_3Cl (10 g), DHPA (1.2× molar equiv. relative to amine), HBTU (1.2× molar equiv. relative to amine), and TEA (2.2× molar equiv. relative to amine). The reaction proceeded for 1.5 h at room temperature. Purification consisted of several precipitations (acidified diethyl ether at –20 °C, acidified methanol at –20 °C, methanol at –20 °C), centrifugation, and decanting. The catechol-modified PEG was vacuum dried overnight to remove residual solvent, dissolved in 12 mM HCl, filtered, transferred into dialysis tubing (3500 Da molecular-weight cut-off (MWCO)), and dialyzed against acidic water (pH 3.5–4.0) for 24 h. The material was then dialyzed against Nanopure H_2O for ≈3 h to minimize the residual acid. The final product, 8cPEGa, was frozen and lyophilized to a white solid (≈90% conjugation).

Hydrogel Formation: 8cPEGa (50 mg) was added to 260.4 µL of Nanopure H_2O of water or buffer. After complete dissolution of the polymer, 62.4 µL of 100 mM, 200 mM, or 300 mM $FeCl_3$ were added to the PEG solution in order to obtain Fe^{3+}:catechol ratios of 1:3, 2:3, and 3:3, respectively. The gelation times were calculated by the inversion method.

Oscillatory Rheometry: Rheometry was performed on an Anton Paar MCR 300 rheometer at 20 °C with a CP 25-2 fixture (25 mm, 2° cone angle). Solutions of 8cPEGa and Fe^{3+} were mixed as above and added as a liquid onto the rheometer baseplate. The fixture was brought down into contact with the gel precursor liquid as quickly as possible. Time tests were performed at 100 Pa shear stress and 10 rad s^{-1}. Frequency sweeps were performed at 10% strain from 100 rad s^{-1} to 0.1 rad s^{-1}. Step-strain experiments were performed at 20% strain, and the stress was monitored for ≈300 s. Strain sweeps were performed at 10 rad s^{-1} from 1% to 1000% strain.

Stability of Gels in Aqueous Environments: The gels were formed in buffers (as above) and allowed to cure for 1.5 h. The samples were submerged in 10 mL of either water or 100 mM EDTA at pH 5. After 24 h, the samples were visually examined in order to determine their stability.

Hydrogel Formation Based on Mussel Processing: Materials were designed by adding 8cPEGa (300 mg) to 1562.4 µL of buffer at pH 3. After complete dissolution of the polymer, 374.4 µL of 200 mM $FeCl_3$ was added to the PEG solution in order to obtain a Fe^{3+}:catechol ratio of 2:3. The solution was quickly added to 4 wells of a polytetrafluoroethylene (PTFE) mold in order to make cylindrical samples. After cross-linking for 24 h, the gels were swelled in 10 mL of buffer (pH 3, 5, 7, or 9) while shaking. After swelling for 24 h, the samples were ready for mechanical testing. This process was repeated in order to create the desired number of samples.

Swelling of "Mussel-Processed" Hydrogels: Swelling experiments were performed by forming samples at pH 3 with a Fe^{3+}:catechol ratio of 2:3. The samples were weighed and swelled in buffer (pH 3, 5, 7, or 9) for 24 h at room temperature while shaking. After removing surface water, the aqueous swelling (AS) was calculated by:

$$\mathrm{AS} = \frac{m_f - m_i}{m_i} \times 100 \quad (1)$$

where m_i and m_f represent the initial and final mass of the hydrogels, respectively. Three trials were performed and the average was reported.

Compressive Testing of "Mussel-Processed" Gels: Two types of compression tests were conducted on a Sintech 20/G mechanical tester. Relaxation experiments were performed with a 250 g load cell on cylindrical samples at a crosshead speed of 40 mm min^{-1} at room temperature. Samples were strained 5%, 10%, or 20%, and the stress was monitored for 100 s. Steady-state moduli were calculated by:

$$\mathrm{Modulus} = \frac{\alpha_{100}}{\varepsilon_{100}} \quad (2)$$

where α_{100} and ε_{100} represent the stress and strain at 100 s, respectively. The extent of relaxation was calculated by:

$$\mathrm{Relaxation} = \frac{\alpha_m - \alpha_{100}}{\alpha_m} \times 100 \quad (3)$$

where α_m and α_{100} represent the maximum stress and stress at 100 s, respectively. The relaxation time was calculated by:

$$\sigma(t) = A_1 + A_2 \exp[-(t)\tau)^{\alpha}] \quad (4)$$

using MATLAB, where $\sigma(t)$ is the stress at time t (Pa), A_1 is the steady-state stress, A_2 is the relaxing stress (Pa), t is the time (s), τ is the relaxation time (s), and α is the expansion coefficient. Three trials were performed, and the average values were reported.

Hysteresis experiments were performed with a 50 lb load cell on cylindrical samples at a crosshead speed of 10 mm min^{-1} at room temperature. The samples were strained to 10%, 20%, 40%, 60%, 70%, and 80% with a 30 s dwell each time the strain returned to 0%.

Supporting Information

Supporting Information is available from the Wiley Online Library or from the author.

Acknowledgements

D.G.B. and D.E.F. contributed equally to this work. The authors thank Dr. Wesley Burghardt, Dr. Sungjin Park, Mark Seniw, and Corey Janczak for insightful discussions. The GPC experiments were performed at Northwestern University's KECK Biophysics facility. The compression experiments made use of Central Facilities supported by the MRSEC program of the National Science Foundation (DMR-1121262) at the

Northwestern University Materials Research Science and Engineering Center. This work was supported by grants from the NIH. D.G.B. and D.E.F. were partially supported by the IBNAM-Baxter Early Career Development Award in Bioengineering and an NIH National Research Service Award from the National Heart, Lung, and Blood Institute (F30HL096292), respectively. N.H.A. thanks the Danish Council for Independent Research, Natural Sciences for a Post-Doctoral Fellowship (No. 272-08-0087), and the University of Chicago Materials Research Science and Engineering Center (DMR 0820054) for the Kadanoff-Rice Postdoctoral Fellowship (2010-12). K.Y.C.L. acknowledges support from the University of Chicago Materials Research Science and Engineering Center (DMR 0820054) and a grant from the NSF (MCB-0920316).

Received: July 10, 2012
Revised: August 29, 2012
Published online: October 2, 2012

[1] H. D. Espinosa, J. E. Rim, F. Barthelat, M. J. Buehler, *Prog. Mater. Sci.* **2009**, *54*, 1059.
[2] N. Huebsch, D. J. Mooney, *Nature* **2009**, *462*, 426.
[3] K. Liu, L. Jiang, *Nano Today* **2011**, *6*, 155.
[4] M. Antonietti, P. Fratzl, *Macromol. Chem. Phys.* **2010**, *211*, 166.
[5] P. Fratzl, *J. R. Soc., Interface* **2007**, *4*, 637.
[6] J. F. V. Vincent, *J. Mater. Res.* **2008**, *23*, 3140.
[7] J. A. Kluge, O. Rabotyagova, G. G. Leisk, D. L. Kaplan, *Trends Biotechnol.* **2008**, *26*, 244.
[8] B. P. Lee, P. B. Messersmith, J. N. Israelachvili, J. H. Waite, *Annu. Rev. Mater. Res.* **2011**, *41*, 99.
[9] M. Heim, D. Keerl, T. Scheibel, *Angew. Chem. Int. Ed.* **2009**, *48*, 3584.
[10] H.-J. Jin, D. L. Kaplan, *Nature* **2003**, *424*, 1057.
[11] F. Vollrath, D. P. Knight, *Nature* **2001**, *410*, 541.
[12] F. Vollrath, D. P. Knight, X. W. Hu, *Proc. R. Soc. London Ser. B* **1998**, *265*, 817.
[13] J. H. Exler, D. Hümmerich, T. Scheibel, *Angew. Chem. Int. Ed.* **2007**, *46*, 3559.
[14] S. Rammensee, U. Slotta, T. Scheibel, A. R. Bausch, *Proc. Natl. Acad. Sci. USA* **2008**, *105*, 6590.
[15] R. J. Stewart, T. C. Ransom, V. Hlady, *J. Polym. Sci., Part B: Polym. Phys.* **2011**, *49*, 757.
[16] T. J. Deming, *Curr. Opin. Chem. Biol.* **1999**, *3*, 100.
[17] H. Lee, N. F. Scherer, P. B. Messersmith, *Proc. Natl. Acad. Sci. USA* **2006**, *103*, 12999.
[18] J. H. Waite, *Int. J. Adhes. Adhes.* **1987**, *7*, 9.
[19] E. Vaccaro, J. H. Waite, *Biomacromolecules* **2001**, *2*, 906.
[20] H. Zhao, J. H. Waite, *Biochemistry* **2006**, *45*, 14223.
[21] M. J. Harrington, J. H. Waite, *J. Exp. Biol.* **2007**, *210*, 4307.
[22] J. Yu, W. Wei, E. Danner, R. K. Ashley, J. N. Israelachvili, J. H. Waite, *Nat. Chem. Biol.* **2011**, *7*, 588.
[23] T. L. Coombs, P. J. Keller, *Aquat. Toxicol.* **1981**, *1*, 291.
[24] M. J. Harrington, A. Masic, N. Holten-Andersen, J. H. Waite, P. Fratzl, *Science* **2010**, *328*, 216.
[25] J. H. Ryu, Y. Lee, W. H. Kong, T. G. Kim, T. G. Park, H. Lee, *Biomacromolecules* **2011**, *12*, 2653.
[26] M. Yu, T. J. Deming, *Macromolecules* **1998**, *31*, 4739.
[27] C. E. Brubaker, H. Kissler, L. J. Wang, D. B. Kaufman, P. B. Messersmith, *Biomaterials* **2010**, *31*, 420.
[28] B. D. Winslow, H. Shao, R. J. Stewart, P. A. Tresco, *Biomaterials* **2010**, *31*, 9373.
[29] K. U. Claussen, R. Giesa, T. Scheibel, H.-W. Schmidt, *Macromol. Rapid Commun.* **2012**, *33*, 206.
[30] N. Holten-Andersen, M. J. Harrington, H. Birkedal, B. P. Lee, P. B. Messersmith, K. Y. C. Lee, J. H. Waite, *Proc. Natl. Acad. Sci. USA* **2011**, *108*, 2651.
[31] D. S. Hwang, H. Zeng, A. Srivastava, D. V. Krogstad, M. Tirrell, J. N. Israelachvili, J. H. Waite, *Soft Matter* **2010**, *6*, 3232.
[32] H. B. Zeng, D. S. Hwang, J. N. Israelachvili, J. H. Waite, *Proc. Natl. Acad. Sci. USA* **2010**, *107*, 12850.
[33] T. H. Anderson, J. Yu, A. Estrada, M. U. Hammer, J. H. Waite, J. N. Israelachvili, *Adv. Funct. Mater.* **2010**, *20*, 4196.
[34] H. Xu, J. Nishida, W. Ma, H. Wu, M. Kobayashi, H. Otsuka, A. Takahara, *ACS Macro Lett.* **2012**, *1*, 457.
[35] E. Mentasti, E. Pelizzetti, *J. Chem. Soc., Dalton Trans.* **1973**, 2605.
[36] E. Mentasti, E. Pelizzetti, G. Saini, *J. Chem. Soc., Dalton Trans.* **1973**, 2609.
[37] M. J. Sever, J. T. Weisser, J. Monahan, S. Srinivasan, J. J. Wilker, *Angew. Chem. Int. Ed.* **2004**, *43*, 448.
[38] G. A. Johnson, D. M. Tramaglini, R. E. Levine, K. Ohno, N.-Y. Choi, S. L-Y. Woo, *J. Orthop. Res.* **1994**, *12*, 796.
[39] W. C. Hayes, L. F. Mockros, *J. Appl. Physiol.* **1971**, *31*, 562.
[40] A. Avdeef, S. R. Sofen, T. L. Bregante, K. N. Raymond, *J. Am. Chem. Soc.* **1978**, *100*, 5362.
[41] B. P. Lee, J. L. Dalsin, P. B. Messersmith, *Biomacromolecules* **2002**, *3*, 1038.
[42] J. J. Wilker, *Curr. Opin. Chem. Biol.* **2010**, *14*, 276.
[43] S. Lv, D. M. Dudek, Y. Cao, M. M. Balamurali, J. Gosline, H. Li, *Nature* **2010**, *465*, 69.
[44] J. B. Thompson, J. H. Kindt, B. Drake, H. G. Hansma, D. E. Morse, P. K. Hansma, *Nature* **2001**, *414*, 773.
[45] G. E. Fantner, T. Hassenkam, J. H. Kindt, J. C. Weaver, H. Birkedal, L. Pechenik, J. A. Cutroni, G. A. G. Cidade, G. D. Stucky, D. E. Morse, P. K. Hansma, *Nat. Mater.* **2005**, *4*, 612.
[46] M. Rief, M. Gautel, F. Oesterhelt, J. M. Fernandez, H. E. Gaub, *Science* **1997**, *276*, 1109.
[47] B. L. Smith, T. E. Schaffer, M. Viani, J. B. Thompson, N. A. Frederick, J. Kindt, A. Belcher, G. D. Stucky, D. E. Morse, P. K. Hansma, *Nature* **1999**, *399*, 761.
[48] G. E. Fantner, E. Oroudjev, G. Schitter, L. S. Golde, P. Thurner, M. M. Finch, P. Turner, T. Gutsmann, D. E. Morse, H. Hansma, P. K. Hansma, *Biophys. J.* **2006**, *90*, 1411.
[49] S. Abdurrahmanoglu, V. Can, O. Okay, *Polymer* **2009**, *50*, 5449.
[50] C. Zhang, A. Aung, L. Liao, S. Varghese, *Soft Matter* **2009**, *5*, 3831.
[51] A. M. Kushner, J. D. Vossler, G. A. Williams, Z. Guan, *J. Am. Chem. Soc.* **2009**, *131*, 8766.
[52] L. Tang, W. Liu, G. Liu, *Adv. Mater.* **2010**, *22*, 2652.
[53] A. Phadke, C. Zhang, B. Arman, C.-C. Hsu, R. A. Mashelkar, A. K. Lele, M. J. Tauber, G. Arya, S. Varghese, *Proc. Natl. Acad. Sci. USA* **2012**, *109*, 4383.
[54] D. Xu, S. L. Craig, *Macromolecules* **2011**, *44*, 7478.